

ON LARGE LAG SMOOTHING FOR HIDDEN MARKOV MODELS*

JEREMIE HOUSSINEAU[†], AJAY JASRA[‡], AND SUMEETPAL S. SINGH[§]

Abstract. In this article we consider the smoothing problem for hidden Markov models. Given a hidden Markov chain $\{X_n\}_{n \geq 0}$ and observations $\{Y_n\}_{n \geq 0}$, our objective is to compute $\mathbb{E}[\varphi(X_0, \dots, X_k)|y_0, \dots, y_n]$ for some real-valued, integrable functional φ and k fixed, $k \ll n$ and for some realization (y_0, \dots, y_n) of (Y_0, \dots, Y_n) . We introduce a novel application of the multilevel Monte Carlo method with a coupling based on the Knothe–Rosenblatt rearrangement. We prove that this method can approximate the aforementioned quantity with a mean square error (MSE) of $\mathcal{O}(\epsilon^2)$ for arbitrary $\epsilon > 0$ with a cost of $\mathcal{O}(\epsilon^{-2})$. This is in contrast to the same direct Monte Carlo method, which requires a cost of $\mathcal{O}(ne^{-2})$ for the same MSE. The approach we suggest is, in general, not possible to implement, so the optimal transport methodology of [A. Spantini, D. Bigoni, and Y. Marzouk, *J. Mach. Learn. Res.*, 19 (2018), pp. 2639–2709; M. Parno, T. Moselhy, and Y. Marzouk, *SIAM/ASA J. Uncertain. Quantif.*, 4 (2016), pp. 1160–1190] is used, which directly approximates our strategy. We show that our theoretical improvements are achieved, even under approximation, in several numerical examples.

Key words. smoothing, multilevel Monte Carlo, optimal transport

AMS subject classifications. 62M05, 62E17

DOI. 10.1137/18M1198004

1. Introduction. Given a hidden Markov chain $\{X_n\}_{n \geq 0}$, $X_n \in \mathsf{X} \subset \mathbb{R}^d$ and observations $\{Y_n\}_{n \geq 0}$, $Y_n \in \mathsf{Y}$, we consider a probabilistic model such that for Borel $A \in \mathcal{X}$, $\mathbb{P}(X_0 \in A) = \int_A f(x)dx$, for every $n \geq 1$, $x_{0:n-1} \in \mathsf{X}^n$

$$(1.1) \quad \mathbb{P}(X_n \in A|x_{0:n-1}) = \int_A f(x_{n-1}, x)dx$$

with dx Lebesgue measure and for Borel $B \in \mathcal{Y}$ and all $n \geq 0$, $(y_{0:n-1}, x_{0:n}) \in \mathsf{Y}^n \times \mathsf{X}^{n+1}$

$$(1.2) \quad \mathbb{P}(Y_n \in B|y_{0:n-1}, x_{0:n}) = \int_B g(x_n, y)dy,$$

where we have used the compact notation $a_{k:n} = (a_k, \dots, a_n)$ for any $k, n \geq 0$ and any sequence $(a_n)_{n \geq 0}$ with the convention that the resulting vector of objects is null if $k > n$. The model defined by (1.1) and (1.2) is termed a hidden Markov model. In this article, given $y_{0:n}$, our objective is to compute $\mathbb{E}[\varphi(X_{0:k})|y_{0:n}]$ for some real-valued, integrable functional φ and k fixed, $k \ll n$, which we refer to as large-lag smoothing. Hidden Markov models and the smoothing problem are found in many real applications, such as finance, genetics, and engineering; see, e.g., [4] and the references therein.

*Received by the editors July 3, 2018; accepted for publication (in revised form) August 30, 2019; published electronically December 3, 2019.

<https://doi.org/10.1137/18M1198004>

Funding: All authors were supported by Singapore Ministry of Education AcRF tier 1 grant R-155-000-182-114. The second author is affiliated with the Risk Management Institute, OR, and Analytics Cluster and the Center for Quantitative Finance at NUS.

[†]Department of Statistics, University of Warwick, Coventry, CV4 7AL, UK (jeremie.houssineau@warwick.ac.uk).

[‡]Computer, Electrical and Mathematical Science and Engineering Division, King Abdullah University of Science and Technology, Thuwal, 23955-6900, Kingdom of Saudi Arabia (ajay.jasra@kaust.edu.sa).

[§]Department of Engineering, University of Cambridge, Cambridge, CB2 1PZ and The Alan Turing Institute, UK (sss40@cam.ac.uk).

The smoothing problem is notoriously challenging. First, $\mathbb{E}[\varphi(X_{0:k})|y_{0:n}]$ is seldom available analytically and hence numerical methods are required. Second, if one wants to compute $\mathbb{E}[\varphi(X_{0:k})|y_{0:n}]$ for several values of n , i.e., potentially recursively, then several of the well-known methods for approximation of $\mathbb{E}[\varphi(X_{0:k})|y_{0:n}]$ can fail. For instance the particle filter (e.g., [8] and the references therein) suffers from the well-known path degeneracy problem (see, e.g., [19]). Despite this, several methods are available for the approximation of $\mathbb{E}[\varphi(X_{0:k})|y_{0:n}]$, such as particle Markov chain Monte Carlo [1] or the PaRIS algorithm [22], which might be considered the current state-of-the-art. The latter algorithm relies on approximating $\mathbb{E}[\varphi(X_{0:k})|y_{0:n^*}]$ for some $n^* < n$ and is then justified on the basis of using *forgetting* properties of the smoother (see, e.g., [4, 7]). We will extend this notion as will be explained below.

The main approach that is followed in this paper is to utilize the multilevel Monte Carlo method (e.g., [10, 13, 12, 15]). Traditional applications of this method are associated to discretizations of continuum problems, but we adopt the framework in a slightly nonstandard way. To describe the basic idea, suppose one is interested in $\mathbb{E}_\pi[\varphi(X)]$ for π a probability, φ real-valued and bounded, but one can only hope to approximate $\mathbb{E}_{\pi_l}[\varphi(X)]$ with π_l a probability (assumed on the same space as π), $l \in \mathbb{N}$, and in some loose sense one has π_l approaches π as l grows. Now, given π_0, \dots, π_L a sequence of increasingly more “precise” probability distributions on the same space, one trivially has

$$(1.3) \quad \mathbb{E}_{\pi_L}[\varphi(X)] = \mathbb{E}_{\pi_0}[\varphi(X)] + \sum_{l=1}^L \{\mathbb{E}_{\pi_l}[\varphi(X)] - \mathbb{E}_{\pi_{l-1}}[\varphi(X)]\}.$$

The approach is now to sample *dependent* couplings of (π_l, π_{l-1}) independently for $1 \leq l \leq L$ and approximate the difference $\mathbb{E}_{\pi_l}[\varphi(X)] - \mathbb{E}_{\pi_{l-1}}[\varphi(X)]$ using Monte Carlo. The term $\mathbb{E}_{\pi_0}[\varphi(X)]$ is also approximated using Monte Carlo with independent and identically distributed (i.i.d.) sampling from π_0 . Then, given a “good enough” coupling and a characterization of the bias, for many practical problems the cost to achieve a prespecified mean square error (MSE) against i.i.d. sampling from π_L and Monte Carlo is significantly reduced. To elaborate the effectiveness of the coupling (as discussed in [11]), the main issue is to approximate (as in (1.3))

$$(1.4) \quad \mathbb{E}_{\pi_l}[\varphi(X)] - \mathbb{E}_{\pi_{l-1}}[\varphi(X)] = \mathbb{E}_{\tilde{\pi}_{l,l-1}}[\varphi(X) - \varphi(Y)],$$

where $\tilde{\pi}_{l,l-1}$ is any probability on the product space (say, $\mathbb{R} \times \mathbb{R}$) of the original probability measures π_l, π_{l-1} with for any measurable $A \subseteq \mathbb{R}$, $\int_{A \times \mathbb{R}} \tilde{\pi}_{l,l-1}(d(x, y)) = \int_A \pi_l(dx)$, $\int_{\mathbb{R} \times A} \tilde{\pi}_{l,l-1}(d(x, y)) = \int_A \pi_{l-1}(dy)$. Now, if one performs i.i.d. sampling from $\tilde{\pi}_{l,l-1}$ to approximate the right-hand side (R.H.S.) of (1.4), the variance of this approximation (of, say, $N \geq 1$ samples) is upper-bounded by a term of the form

$$\frac{\|\varphi\|_{\text{Lip}}}{N} \mathbb{E}_{\tilde{\pi}_{l,l-1}}[|X - Y|^2],$$

where we assume φ is Lipschitz, and $|\varphi(x) - \varphi(y)| \leq \|\varphi\|_{\text{Lip}}|x - y|$. Now, the gain of MLMC is possible if the coupling can strongly correlate X, Y . In the case above, we know that the optimal coupling is that w.r.t. squared Wasserstein distance.

We leverage the idea of MLMC where the “level” l corresponds to the time parameter and L is some chosen n^* , so as to achieve a given level of bias. The main issue is then how to sample from couplings which are good enough. We show that, as elaborated on above, when $d = 1$ (the dimension of the hidden state) using the optimal coupling, in terms of squared Wasserstein distance, can yield significant

improvements over the case where one directly approximates $\mathbb{E}[\varphi(X_{0:k})|y_{0:n}]$ with Monte Carlo and i.i.d sampling from the smoother. That is, for $\epsilon > 0$ given, to achieve an MSE of $\mathcal{O}(\epsilon^2)$, the cost is $\mathcal{O}(\epsilon^{-2})$, whereas for the ordinary Monte Carlo method the cost is $\mathcal{O}(n\epsilon^{-2})$. The same conclusion with $d > 1$ can be achieved using the Knothe–Rosenblatt rearrangement. The main issue with our approach is that it cannot be implemented for most problems of practical interest. However, using the transport methodology in [26], it can be approximated. We show that in numerical examples our predicted theory is verified, even under this approximation. We also compare our method directly with PaRIS, showing substantial improvement in terms of cost for a given level of MSE. Note that the transport methodology used here differs fundamentally from the “particle flow” methods discussed in [6, 3, 14], where samples from a base probability distributions are moved using an ordinary differential equation adapted to the target distribution.

This article is structured as follows. In section 2 we detail our approach and theoretical results. In section 3 we demonstrate how our approach can be implemented in practice. In section 4 we give our numerical examples. Section 5 summarizes the article. The appendix includes the assumptions, technical results, and proofs of our main results.

1.1. Notation. Let (X, \mathcal{X}) be a measurable space. For $\varphi : X \rightarrow \mathbb{R}$ we write $\mathcal{B}_b(X)$ and $\text{Lip}(X)$ as the collection of bounded measurable and Lipschitz functions, respectively. For $\varphi \in \mathcal{B}_b(X)$, we write the supremum norm $\|\varphi\| = \sup_{x \in X} |\varphi(x)|$. For $\varphi \in \mathcal{B}_b(X)$, $\text{Osc}(\varphi) = \sup_{(x,y) \in X \times X} |\varphi(x) - \varphi(y)|$, and we write $\text{Osc}_1(X)$ for the set of functions φ on X such that $\text{Osc}(\varphi) = 1$. For $\varphi \in \text{Lip}(X)$, we write the Lipschitz constant $\|\varphi\|_{\text{Lip}}$. $\mathcal{P}(X)$ denotes the collection of probability measures on (X, \mathcal{X}) . For a measure μ on (X, \mathcal{X}) and a $\varphi \in \mathcal{B}_b(X)$, the notation $\mu(\varphi) = \int_X \varphi(x) \mu(dx)$ is used. Letting $K : X \times \mathcal{X} \rightarrow [0, 1]$ be a Markov kernel and μ be a measure, then we use the notation $\mu K(dy) = \int_X \mu(dx) K(x, dy)$ and for $\varphi \in \mathcal{B}_b(X)$, $K(\varphi)(x) = \int_X \varphi(y) K(x, dy)$. For a sequence of Markov kernels K_1, \dots, K_n we write

$$K_{1:n}(x_0, dx_n) = \int_{X^{n-1}} \prod_{p=1}^n K_p(x_{p-1}, dx_p).$$

For $\mu, \nu \in \mathcal{P}(X)$, the total variation distance is written $\|\mu - \nu\|_{\text{tv}} = \sup_{A \in \mathcal{X}} |\mu(A) - \nu(A)|$. For $A \in \mathcal{X}$ the indicator is written $\mathbb{I}_A(x)$. \mathcal{U}_A denotes the uniform distribution on the set A . $\mathcal{N}(a, b)$ is the one-dimensional Gaussian distribution of mean a and variance b .

2. Model and approach. We are given a hidden Markov model (HMM) and we seek to compute

$$\mathbb{E}_{\pi_{n,0}}[\varphi(X_0)|y_{0:n}] = \frac{\int_{X^{n+1}} \varphi(x_0) \prod_{p=0}^n g(x_p, y_p) f(x_{p-1}, x_p) dx_{0:n}}{\int_{X^{n+1}} \prod_{p=0}^n g(x_p, y_p) f(x_{p-1}, x_p) dx_{0:n}},$$

where $f(x_{-1}, x_0) := f(x_0)$ and for ease of simplicity we suppose that $\varphi \in \mathcal{B}_b(X) \cap \text{Lip}(X)$ and X is a compact subspace of the real line. $\pi_{n,0}$ is the probability density (we also use the same symbol for probability measure) of the smoother given n observations at the coordinate at time 0. That is,

$$\pi_{n,0}(x_0|y_{0:n}) \propto \int_{X^n} \prod_{p=0}^n g(x_p, y_p) f(x_{p-1}, x_p) dx_{1:n}.$$

Let $0 < n^* < n$ be fixed, and then we propose to consider

$$\mathbb{E}_{\pi_{n^*,0}}[\varphi(X_0)|y_{0:n^*}] = \mathbb{E}_{\pi_{0,0}}[\varphi(X_0)|y_0] + \sum_{p=1}^{n^*} \{\mathbb{E}_{\pi_{p,0}}[\varphi(X_0)|y_{0:p}] - \mathbb{E}_{\pi_{p-1,0}}[\varphi(X_0)|y_{0:p-1}]\}.$$

2.1. Case $\mathbf{X} \subset \mathbb{R}$. Let us denote the cumulative distribution function (CDF) of $\pi_{p,0}$ as $\Pi_{p,0}$. An approximation of $\mathbb{E}_{\pi_{p,0}}[\varphi(X_0)|y_{0:p}] - \mathbb{E}_{\pi_{p-1,0}}[\varphi(X_0)|y_{0:p-1}]$ is

$$\frac{1}{N_p} \sum_{i=1}^{N_p} [\varphi(\Pi_{p,0}^{-1}(U^i)) - \varphi(\Pi_{p-1,0}^{-1}(U^i))],$$

where for $i \in \{1, \dots, N_p\}$, $U^i \stackrel{\text{i.i.d.}}{\sim} \mathcal{U}_{[0,1]}$ and $\Pi_{p,0}^{-1}$ is the (generalized) inverse CDF of $\Pi_{p,0}$. If we do this independently for each $p \in \{1, \dots, n\}$ and use an independent estimator $\frac{1}{N_0} \sum_{i=1}^N \varphi(\Pi_0^{-1}(U^i))$ for $\mathbb{E}_{\pi_{0,0}}[\varphi(X_0)|y_0]$ one can estimate $\mathbb{E}[\varphi(X_0)|y_{0:n}]$. The utility of the coupling is that it is optimal in terms of 2-Wasserstein distance. We have the following result, where the assumption and proof are in the appendix.

THEOREM 2.1. *Assume (A1). Then there exists $\rho \in (0, 1)$, $C < +\infty$ such that for any $\varphi \in \mathcal{B}_b(\mathbf{X}) \cap \text{Lip}(\mathbf{X})$, $n^* \geq p \geq 1$, $N_p \geq 1$, we have*

$$\mathbb{V}\text{ar}\left[\frac{1}{N_p} \sum_{i=1}^{N_p} [\varphi(\Pi_{p,0}^{-1}(U^i)) - \varphi(\Pi_{p-1,0}^{-1}(U^i))]\right] \leq \frac{C\rho^{p-1}\|\varphi\|_{\text{Lip}}^2}{N_p}.$$

The main implication of the result is the following. In the approach to be considered later in this paper the cost of computing (an approximation of) $(\Pi_{p,0}^{-1}, \Pi_{p-1,0}^{-1})$ is $\mathcal{O}(1)$ per time step. So the cost of this method is $C(n^* + \sum_{p=0}^{n^*} N_p)$. Thus the MSE and cost associated with this algorithm are (at most in the first case)

$$C(\|\varphi\|^2 \vee \|\varphi\|_{\text{Lip}}^2) \left(\frac{1}{N_0} + \sum_{p=1}^{n^*} \frac{\rho^{p-1}}{N_p} + \rho^{2n} \right)$$

and

$$(2.1) \quad C \left(n^* + \sum_{p=0}^{n^*} N_p \right).$$

Let $\epsilon > 0$ be given. To achieve an MSE of $\mathcal{O}(\epsilon^2)$ we can choose $n^* = |\log(\epsilon)/\log(\rho)|$ (here we of course mean $n^* = \lceil |\log(\epsilon)/\log(\rho)| \rceil$, but this is omitted for simplicity) and $N_p = \epsilon^{-2}(p+1)^{-1-\delta}$ for any $\delta > 0$ yields that the associated cost is $\mathcal{O}(\epsilon^{-2})$. If one just approximates $\mathbb{E}_{\pi_{n,0}}[\varphi(X_0)|y_{0:n}]$ using

$$\frac{1}{N} \sum_{i=1}^N \varphi(\Pi_{n,0}^{-1}(U^i)),$$

then to achieve an MSE of $\mathcal{O}(\epsilon^2)$ the cost would be $\mathcal{O}(n\epsilon^{-2})$, which is considerably larger if n is large. That is, the cost of the ML approach is essentially $\mathcal{O}(1)$ w.r.t. n . If one stops at $n^* = |\log(\epsilon)/\log(\rho)|$ and uses the estimate

$$\frac{1}{N} \sum_{i=1}^N \varphi(\Pi_{n^*,0}^{-1}(U^i))$$

to achieve an MSE of $\mathcal{O}(\epsilon^2)$, the cost is $\mathcal{O}(\epsilon^{-2}|\log(\epsilon)|)$. A similar approach can show that these results are even true when smoothing for $\mathbb{E}[\varphi(X_{0:k})|y_{0:n}]$ for k fixed (and hence $\mathbb{E}[\varphi(X_{s:s+k})|y_{0:n}]$). The strategy of choosing n^* and $N_{0:n^*}$ detailed above is the one used throughout the paper. Note that in practice, we do not know ρ , so we choose a value such as $\rho = 0.8$ which should lead to an n^* which is large enough. This is also the reason for setting $N_p = \epsilon^{-2}(p+1)^{-1-\delta}$ and not $N_p = \epsilon^{-2}(\rho^{1/2})^{p-1}$, say.

It is remarked that the compactness of X could potentially be removed by using Kellerer's extension of the Kantorovich–Rubenstein theorem (see [9] for a summary) along with the techniques of [17]. Such an extension is mainly of a technical nature and is not required in the continuing exposition. We now establish that the construction here can be extended to the case $X \subset \mathbb{R}^d$.

2.2. Case $X \subset \mathbb{R}^d$. We consider the Knothe–Rosenblatt rearrangement, which is assumed to exist (see, e.g., [26]). For simplicity of notation, we set $X = E^d$ for some compact $E \subset \mathbb{R}$. Denote by $\Pi_{p,0}(\cdot|x_{1:j})$ the conditional CDF of $\pi_{p,0}(x_{j+1}|x_{1:j})$ with $1 \leq j \leq d-1$. Note that here we are dealing with the d -dimensional coordinate at time zero and we are considering conditioning on the first j of these dimensions. Then to approximate $\mathbb{E}_{\pi_{p,0}}[\varphi(X_0)|y_{0:p}] - \mathbb{E}_{\pi_{p-1,0}}[\varphi(X_0)|y_{0:p-1}]$, sample $U_{1:d}^1, \dots, U_{1:d}^{N_p}$, where for $i \in \{1, \dots, N_p\}$, $U_{1:d}^i \stackrel{\text{i.i.d.}}{\sim} \mathcal{U}_{[0,1]^d}$. Then we have the estimate for $\varphi \in \mathcal{B}_b(X) \cap \text{Lip}(X)$

$$\frac{1}{N_p} \sum_{i=1}^{N_p} [\varphi(\xi_{p,d}^i) - \varphi(\xi_{p-1,d}^i)],$$

where for ease of notation, we have set $\xi_{p,1}^i = \Pi_{p,0}^{-1}(U_1^i)$ (resp., $\xi_{p-1,1}^i = \Pi_{p-1,0}^{-1}(U_1^i)$) and $\xi_{p,j}^i = (\xi_{p,1}^i, \dots, \xi_{p,j-1}^i, \Pi_{p,0}^{-1}(U_j^i|\xi_{p,j-1}^i))$, $2 \leq j \leq d$ (resp., $\xi_{p-1,j}^i = (\xi_{p-1,1}^i, \dots, \xi_{p-1,j-1}^i, \Pi_{p-1,0}^{-1}(U_j^i|\xi_{p-1,j-1}^i))$, $2 \leq j \leq d$). We have the following result, whose proof and assumptions are in the appendix.

THEOREM 2.2. *Assume (A1–2). Then there exists $\rho \in (0,1)$, $C < +\infty$ such that for any $\varphi \in \mathcal{B}_b(X) \cap \text{Lip}(X)$, $n^* \geq p \geq 1$, $N_p \geq 1$, we have*

$$\text{Var}\left[\frac{1}{N_p} \sum_{i=1}^{N_p} [\varphi(\xi_{p,d}^i) - \varphi(\xi_{p-1,d}^i)]\right] \leq \frac{C\rho^{p-1}\|\varphi\|_{\text{Lip}}^2}{N_p}.$$

As will be detailed in the following section and in particular in Algorithm 3.1, it is often more convenient in practice to use the standard normal distribution instead of the uniform distribution as a base distribution. The only difference is that samples from the standard normal distribution first have to be mapped through the corresponding CDF before taking the inverse image through the CDF of interest, e.g., $\Pi_{p,0}^{-1}(\cdot|x_{1:j})$ for some $p \geq 0$ and some $1 \leq j \leq d-1$.

We end this section with some remarks. First, the MLMC strategy could be debiased w.r.t. the time parameter using the trick in [25], which is a straightforward extension. One minor issue with this methodology is that the variance can blow up in some scenarios. Second, the idea of using the approach in [25], when approximating $\mathbb{E}[\varphi(X_{0:n})|y_{0:n}]$, has been adopted in [16]. The authors use a conditional version of the coupled particle filter (e.g., [5, 18]) to couple smoothers, versus the optimal Wasserstein coupling. The goal in [16] is unbiased estimation, which is complementary to ideas in this article, where we focus upon reducing the cost of large lag smoothing.

3. Transport methodology.

3.1. Standard approach. The basic principle of the transport methodology introduced in [26] is to determine a mapping T relating a base distribution η , e.g., the normal distribution, to a potentially sophisticated target distribution $\tilde{\pi}$ related to the problem of interest. The distribution η should be easy to sample from so that, given the map T , we can obtain samples from $\tilde{\pi}$ by simply mapping samples from η via T . More precisely, the considered mapping T is characterized by

$$T_{\#}\eta(x) = \eta(T^{-1}(x))|\det \nabla T^{-1}(x)| = \tilde{\pi}(x),$$

that is, the *push-forward* distribution of η by T is $\tilde{\pi}$. Such a mapping can be approximated using deterministic or stochastic optimization methods. However, the underlying optimization problem is only amenable when the space on which $\tilde{\pi}$ is defined is of a low dimension, e.g., up to 4. This is not the case in general for the smoothing distributions introduced in the previous sections, especially as the number of observations increases. This is addressed in [26] by identifying the dependence structure between the random variables of interest. In particular, for a hidden Markov model on \mathbb{R}^d , it is possible to decompose the problem into transport maps of dimension $2d$, which does not depend on the number n of observations that define the smoother. The problem at time p can be solved by introducing a mapping T_p of the form

$$T_p(x_p, x_{p+1}) = \begin{bmatrix} T_p^0(x_p, x_{p+1}) \\ T_p^1(x_{p+1}) \end{bmatrix},$$

which will transform the $2d$ -dimensional base distribution η_{2d} into a target distribution related to the considered hidden Markov model, as detailed below. This target distribution can be expressed as

$$\tilde{\pi}_p(x_p, x_{p+1}) \propto \eta_d(x_p) f(T_{p-1}^1(x_p), x_{p+1}) g(x_{p+1}, y_{p+1})$$

for any $p > 0$, which can be seen to be related to the 1-lag smoother. When $p = 0$, we simply define $\tilde{\pi}_0(x_0, x_1) = f(x_0) f(x_0, x_1) g(x_0, y_0) g(x_1, y_1)$. The base distribution η_{2d} (resp., η_d) is the standard normal distribution of dimension $2d$ (resp., d). The mapping T_p can be embedded into the $2d(n+1)$ -dimensional identity mapping as

$$\bar{T}_p(x_0, \dots, x_n) = (x_0, \dots, x_{p-1}, T_p^0(x_p, x_{p+1}), T_p^1(x_{p+1}), x_{p+2}, \dots, x_n)^t$$

with \cdot^t denoting the matrix transposition. It follows that

$$\mathbf{T}_n = \bar{T}_0 \circ \dots \circ \bar{T}_n$$

is the map such that the pushforward $(\mathbf{T}_n)_{\#}\eta_{d(n+1)}$ is equal to the probability density function of the smoother at time n . Obtaining samples from the smoothing distribution is then straightforward: it suffices to sample from $\eta_{d(n+1)}$ and to map the obtained sample via \mathbf{T}_n .

Even in low dimension, the optimization problem underlying the computation of the transport maps of interest is not trivial. One first has to consider an appropriate parametrization of these maps, e.g., via polynomial representations. The parameters of the considered representation then have to be determined using the following optimization problem:

$$(3.1) \quad T_p^* = \operatorname{argmin}_T -\mathbb{E} \left[\log \tilde{\pi}_p(T(X)) + \log (\det \nabla T(X)) - \log \eta_{2d}(X) \right],$$

where the minimum is taken over the set of monotone increasing lower-triangular maps. This minimization problem can be solved numerically by considering a parametrized family of maps and deterministic or stochastic optimization methods. Let T be any acceptable map in the minimization (3.1) and denote by $T^{(i)}$ the i th component of T , which only depends on the i th first variables, $i \in \{1, \dots, 2d\}$, then the considered parametrization can be expressed as

$$T^{(i)}(x_1, \dots, x_i) = a_i(x_1, \dots, x_{i-1}) + \int_0^{x_i} b_i(x_1, \dots, x_{i-1}, t)^2 dt$$

for some real-valued functions a_i and b_i on \mathbb{R}^{i-1} and \mathbb{R}^i , respectively. It is assumed that the functions $x_j \mapsto a_i(x_1, \dots, x_{i-1})$ and $x_j \mapsto b_i(x_1, \dots, x_{i-1}, t)$ are probabilists' Hermite functions [2] extended with constant and linear components for any $j \leq i-1$, and the function $t \mapsto b_i(x_1, \dots, x_{i-1}, t)$ is also a probabilists' Hermite function which is only extended with a constant component. In particular, these functions take the form

$$\begin{aligned} a_i(x_1, \dots, x_{i-1}) &= \sum_{k=1}^{2d(o_{\text{map}}+1)} c_k \Phi_k(x_1, \dots, x_{i-1}), \\ b_i(x_1, \dots, x_{i-1}, t) &= \sum_{k=1}^{2d o_{\text{map}}} c'_k \Psi_k(x_1, \dots, x_{i-1}, t) \end{aligned}$$

with o_{map} the map order, with $\{c_k\}_{k \geq 1}$ and $\{c'_k\}_{k \geq 1}$ some collections of real coefficients, and with Φ_k and Ψ_k basis functions based on the above-mentioned probabilists' Hermite functions. The expectation in (3.1) is then approximated using a Gauss quadrature of order o_{exp} in each dimension and the minimization is solved via the Newton algorithm using the conjugate-gradient method for each step.

The desired function T_p can be recovered through the relation

$$\begin{aligned} (3.2) \quad T_p((x_{p,1}, \dots, x_{p,d}), (x_{p+1,1}, \dots, x_{p+1,d})) \\ = (S_\sigma \circ T_p^* \circ S_\sigma)(x_{p,1}, \dots, x_{p,d}, x_{p+1,1}, \dots, x_{p+1,d}), \end{aligned}$$

where $\sigma = (2d, 2d-1, \dots, 1)$ and S_σ is the linear map corresponding to the permutation matrix of σ , which verifies $S_\sigma^{-1} = S_\sigma$.

3.2. Fixed-point smoothing with transport maps. The approach described in section 3.1 allows for obtaining samples from the distribution $\pi_{n,0}$ of X_0 given $(Y_0, \dots, Y_n) = (y_0, \dots, y_n)$ by simply retaining the first d components of samples from $\eta_{d(n+1)}$ after mapping them through T_n . However, the computational cost associated with the mapping of samples by T_n increases with n , making the complexity of the method of the order $\mathcal{O}(n^2)$.

This can, however, be addressed by considering X_0 as a parameter and by only propagating the transport map corresponding to the posterior distribution of (X_0, X_n) . This approach has been suggested in [26, section 7.4]. We assume in the remainder of this section that observations start at time step 1 instead of 0. When considering X_0 as a parameter, the elementary transport maps take the form

$$T_p(x_0, x_p, x_{p+1}) = \begin{bmatrix} T_p^{X_0}(x_0) \\ T_p^0(x_0, x_p, x_{p+1}) \\ T_p^1(x_0, x_{p+1}) \end{bmatrix},$$

and the corresponding target distributions become

$$\tilde{\pi}_1(x_0, x_1, x_2) \propto p_0(x_0)f(x_0, x_1)f(x_1, x_2)g(x_1, y_1)g(x_2, y_2)$$

and

$$\tilde{\pi}_p(x_0, x_p, x_{p+1}) \propto \eta_{2d}(x_0, x_p)f(T_{p-1}^1(x_0, x_p), x_{p+1})g(x_{p+1}, y_{p+1})$$

for any $p > 1$. The transport map associated with the posterior distribution of (X_0, X_n) is

$$\hat{T}_n(x_0, x_n) = \begin{bmatrix} T_1^{X_0} \circ \cdots \circ T_{n-1}^{X_0}(x_0) \\ T_{n-1}^1(x_0, x_n) \end{bmatrix}.$$

By recursively approximating the composition $T_1^{X_0} \circ \cdots \circ T_{n-1}^{X_0}$ by a single map, the computation of samples from the posterior distribution of X_0 becomes linear in time. The pseudocode for this approach is given in Algorithm 3.1.

Algorithm 3.1 Multilevel transport.

```

1: Input:  $\epsilon, \delta, \rho$ 
2: Output: estimate  $\hat{X}_0$  of  $\varphi(X_0) \mid y_{0:n^*}$ 
3:  $n^* = \log(\epsilon)/\log(\rho)$ 
4: for  $p = 1, \dots, n^*$  do
5:   if  $p = 1$  then
6:      $\tilde{\pi}_p(x_0, x_1, x_2) \propto p_0(x_0)f(x_0, x_1)f(x_1, x_2)g(x_1, y_1)g(x_2, y_2)$ 
7:   else
8:      $\tilde{\pi}_p(x_0, x_p, x_{p+1}) \propto \eta_{2d}(x_0, x_p)f(T_{p-1}^1(x_0, x_p), x_{p+1})g(x_{p+1}, y_{p+1})$ 
9:      $\triangleright T_{p-1}^1$  is the second component of  $\hat{T}_{p-1}$ 
10:  end if
11:   $\eta = \mathcal{N}(\mathbf{0}_{2d}, \mathbf{I}_{2d})$ 
12:   $\hat{T}_p = \text{FilteringDistributionTransportMap}(\eta, \tilde{\pi}_p)$ 
13:   $\triangleright$  Compute transport map from  $\eta$  to the law of  $(X_0, X_p) \mid y_{1:p}$  based on  $\tilde{\pi}_p$ 
14:   $N_p = \epsilon^{-2}(p+1)^{-1-\delta}$   $\triangleright$  Compute the number of samples
15:  for  $i = 1, \dots, N_p$  do
16:     $S \sim \eta$ 
17:     $\xi_p^i = \hat{T}_p(S)$ 
18:    if  $p = 1$  then
19:       $\zeta_p^i = \varphi(\xi_p^{i,1:d})$   $\triangleright$  Map the first  $d$  components of  $\xi_p^i$  through  $\varphi$ 
20:    else
21:       $\xi_{p-1}^i = \hat{T}_{p-1}(S)$ 
22:       $\zeta_p^i = \varphi(\xi_p^{i,1:d}) - \varphi(\xi_{p-1}^{i,1:d})$ 
23:    end if
24:  end for
25:   $\hat{X}_0 \leftarrow \hat{X}_0 + \frac{1}{N_p} \sum_{i=1}^{N_p} \zeta_p^i$ 
26: end for

```

4. Case studies.

4.1. Linear Gaussian.

4.1.1. Theoretical result. The results in section 2 do not apply to the linear Gaussian case. We extend our results to this scenario. We assume that the dynamical

and observations models are one-dimensional as well as linear and Gaussian such that the state and observation random variables at time n can be defined as

$$(4.1a) \quad X_n|x_{n-1} \sim \mathcal{N}(\alpha x_{n-1}, \beta^2), \quad n \geq 1,$$

$$(4.1b) \quad Y_n|x_n \sim \mathcal{N}(x_n, \tau^2), \quad n \geq 0,$$

and $X_0 \sim \mathcal{N}(0, \sigma^2)$ for some $\alpha \in \mathbb{R}$ and some $\beta, \sigma, \tau > 0$. We have the following result, whose proof is in the appendix.

THEOREM 4.1. *Assuming that $\text{Var}(X_p | y_{0:p}) \approx \gamma^2$ for all p large enough, it holds that*

$$\text{Var}\left[\frac{1}{N_p} \sum_{i=1}^{N_p} [\Pi_{p,0}^{-1}(U^i) - \Pi_{p-1,0}^{-1}(U^i)]\right] = \mathcal{O}\left(\frac{1}{N_p} \left(\alpha + \frac{\beta^2}{\alpha \gamma^2}\right)^{-2p}\right).$$

Theorem 4.1 shows that, under assumptions on the parameters of the model, the variance of the approximated multilevel term at level p tends to 0 exponentially fast in p and with an order of $1/N_p$ for the number of samples. This theorem also indicates that the behavior depends on all the parameters in the model, although implicitly in τ . For instance, if $\beta \gg \tau$, then one can consider $\gamma = \tau$ in the above expression. The assumption about the variance of the filter can be justified in terms of reachability and observability of the system [20].

This rate can get extremely beneficial for the proposed approach when β is large and γ is small, but it can also make it of little use in the opposite case. This does not come as a surprise since a large β means that the initial condition is quickly forgotten so that obtaining a high number of samples from the smoother $\pi_{p,0}$ for large p would be inefficient, whereas small values of β incur a much higher dependency between the initial state and the observations at different time steps.

4.1.2. Numerical results. The performance of the proposed method is first assessed in the linear-Gaussian case where an analytical solution of the fixed-point smoothing problem is available, this solution being known as the Rauch–Tung–Striebel smoother [24]. More specifically, we consider the model (4.1) with $X_0 \sim \mathcal{N}(1, \sigma^2)$, $\sigma = 2$, and $\alpha = \beta = \tau = 1$. The transport maps of interest are approximated¹ to the order $o_{\text{map}} = 3$ while the expectation is approximated to the order $o_{\text{exp}} = 5$ and the minimization is performed with a tolerance of 10^{-4} . The number of samples at each time step as well as the time horizon n^* is computed according to the method proposed in section 2.1 with different values for the parameter ϵ and with $\rho = 0.8$. The performance of the proposed method is compared against the PaRIS algorithm introduced in [22] using the observations y_1, \dots, y_{50} with a varying number N of samples and with $\tilde{N} = 2$ terms for the propagation of the estimate of X_0 . In the simulations, it always holds that $n^* \leq 50$ to ensure the fairness of the comparison. The criteria for performance assessment is the MSE at the final time step, defined as

$$\frac{1}{M} \sum_{i=1}^M (\hat{x}_i - x^*)^2,$$

where M is the number of Monte Carlo simulations, \hat{x}_i is the estimate of $X_0 | y_{1:n^*}$ (with $n^* = 50$ for the PaRIS algorithm), and x^* is the corresponding estimate given by the Rauch–Tung–Striebel smoother.

¹The solver used for the determination of the transport maps is the one provided at <http://transportmaps.mit.edu/docs/index.html>.

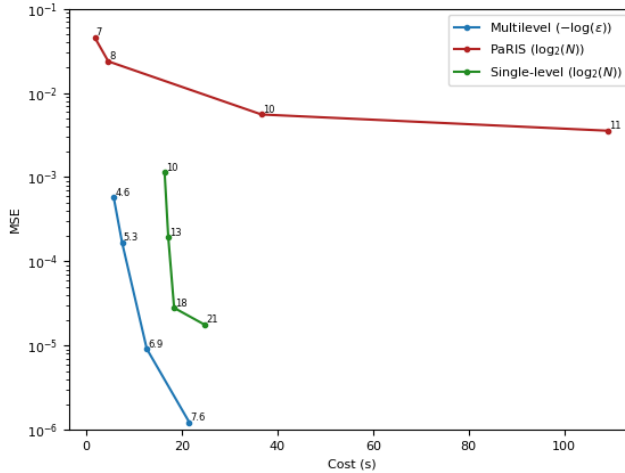


FIG. 1. Performance of the proposed method against the PaRIS algorithm and the single-level transport-map approach for the linear-Gaussian model, averaged over 100 Monte Carlo simulations. The reference for the computation of the MSE is the Rauch-Tung-Striebel smoother. The displayed cost for the multilevel approach includes the computation of the transport maps.

The values of the MSE at the final time obtained in simulations are shown in Figure 1, where the proposed approach displays smaller errors than the PaRIS algorithm for different values of ϵ and N . The comparison is also made with a single-level transport-map approach, i.e., without the multilevel decomposition, for different numbers of samples. The advantage when representing the probability distributions of interest with transport maps is that the computational effort required to obtain a sample is extremely limited once the maps have been determined. For instance, the highest and lowest considered values of ϵ in Figure 1 correspond to $N_1 = 1250$ and $N_1 = 500,000$ samples, respectively, which induces a comparatively small increase in computational time.

In this linear-Gaussian case, using maps of order $o_{\text{map}} < 3$ would have been sufficient, but this would have been equivalent to making an assumption on the type of distribution considered for the proposed algorithm whereas the PaRIS algorithm makes no such assumption. The reason for choosing specifically $o_{\text{map}} = 3$ is that this value was found to be sufficient for nonlinear models as in the next section.

4.2. Stochastic volatility model. In order to further demonstrate the performance of the proposed approach, the assessment conducted in the previous section is applied to the estimation of $X_0 | y_{1:n^*}$ in a nonlinear case. A stochastic volatility model is considered with

$$\begin{aligned} X_n &= \mu + \phi(X_{n-1} - \mu) + V_n, \quad n \geq 1, \quad X_0 \sim \mathcal{N}\left(\mu, \frac{1}{1-\phi^2}\right), \\ Y_n &= W_n \exp\left(\frac{1}{2}X_n\right), \quad n \geq 0, \end{aligned}$$

with $V_n \sim \mathcal{N}(0, \beta^2)$ and $W_n \sim \mathcal{N}(0, 1)$, where $\mu = -0.5$, $\phi = 0.95$, and $\beta = 0.25$. In the absence of an analytical solution, the reference is determined by the PaRIS algorithm with $N = 2^{14}$ samples. Since the observation process of this model is generally less informative than the one of the Gaussian model, the PaRIS algorithm

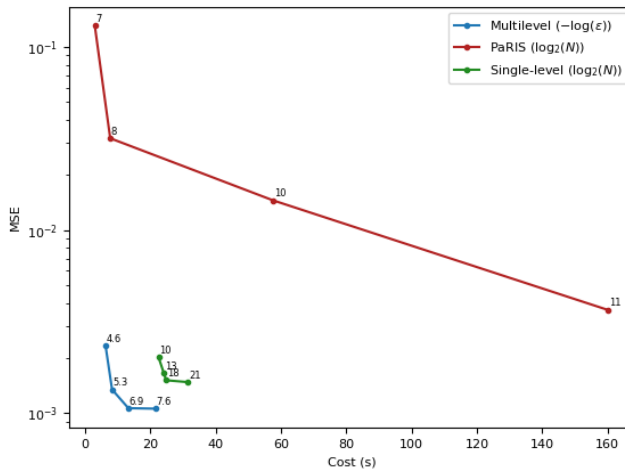


FIG. 2. Performance of the proposed method against the PaRIS algorithm and the single-level transport-map approach for the stochastic volatility model, averaged over 100 Monte Carlo simulations. The reference for the computation of the MSE is the PaRIS algorithm with 2^{14} samples. The displayed cost for the multilevel approach includes the computation of the transport maps.

is given the observations up to the time step 50 and, similarly, it is ensured that $n^* \leq 50$ for the proposed approach. The other parameters are the same as in the linear-Gaussian case, that is, maps of order $o_{\text{map}} = 3$ are used, the expectation is approximated to the order $o_{\text{exp}} = 5$, and the minimization is performed with a tolerance of 10^{-4} .

The MSE at the final time obtained for the two considered methods is shown in Figure 2. Once again, the error for the proposed approach is lower than for the PaRIS algorithm although the difference is less significant. In particular, the gain in accuracy between the lowest and the second lowest value of ϵ seem to indicate that simply increasing the number of samples would not allow for reducing the error much further. However, increasing the order of the transport maps or decreasing the tolerance in the optimization could further reduce the error, although with a significantly higher computational cost.

The computational costs obtained for the two models considered in simulations are shown in Figure 3 for different values of ϵ . These results confirm the order $\mathcal{O}(\epsilon^{-2})$ that was predicted in section 2.

5. Summary. In this article we have considered large lag smoothing for HMMs, using the MLMC method. We showed that under an optimal coupling when the hidden state is in dimension 1 or higher, but on a compact space, that, essentially, the cost can be decoupled from the time parameter of the smoother. As this optimal method is not possible in practice, we showed how it could be approximated and established numerically that our theory still holds in this approximated case. Several extensions to the work are possible: first, to extend our theoretical results to the case of the approximated coupling, and second, to investigate whether the coupling used in [16] can also yield, theoretically, the same improvements that have been seen in the work in this article.

Appendix A. Variance proofs. We write the density (or probability measure) of the smoother, at time p , on the coordinate at time zero as $\pi_{p,0}$ and the associated

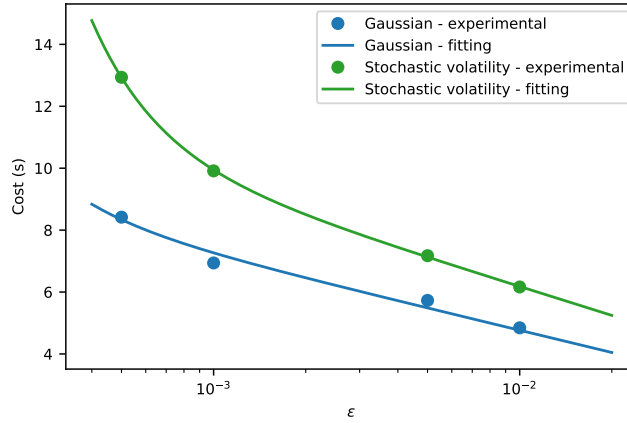


FIG. 3. Computational cost as a function of ϵ , averaged over 100 Monte Carlo simulations. The fitted curves are based on a function of the form $\epsilon \mapsto -a\epsilon^{-2} - b\log(\epsilon)$, with a and b some parameters, which is justified by the form of the cost (2.1).

CDF as $\Pi_{p,0}$ (with generalized inverse $\Pi_{p,0}^{-1}$). Recall that throughout \mathbf{X} is a compact subspace of \mathbb{R}^d . Throughout the observations are fixed and often omitted from the notation. The appendix gives our main assumptions, followed by a technical lemma (Lemma A.1) which features some technical results used in the proofs. Then the proof of Theorem 2.1 is given. The appendix is concluded by a second technical lemma (Lemma A.2) followed by the proof of Theorem 2.2.

(A1) There exists $0 < \underline{C} < \bar{C} < +\infty$ such that

$$\begin{aligned} \inf_{x \in \mathbf{X}} g(x, y_0) f(x) \wedge \inf_{p \geq 1} \inf_{(x, x') \in \mathbf{X}^2} g(x', y_p) f(x, x') &\geq \underline{C}, \\ \sup_{x \in \mathbf{X}} g(x, y_0) f(x) \vee \sup_{p \geq 1} \sup_{(x, x') \in \mathbf{X}^2} g(x', y_p) f(x, x') &\leq \bar{C}. \end{aligned}$$

(A2) There exists $C < +\infty$ such that for every $(x, x') \in \mathbf{X}^2$

$$\begin{aligned} |g(x, y_0) - g(x', y_0)| &\leq C|x - x'|, \\ \sup_{z \in \mathbf{X}} |f(x, z) - f(x', z)| &\leq C|x - x'|, \\ |f(x) - f(x')| &\leq C|x - x'|. \end{aligned}$$

Below $\pi_{p,0}(\cdot|x_{1:j})$ denotes the probability of the $(j+1)$ th coordinate of the smoother at time 0, given the first j coordinates at time 0, and conditional upon the observations up to time p .

LEMMA A.1. *Assume (A1–2). Then there exists $(C, C') \in (0, \infty)^2$, $\rho \in (0, 1)$ such that*

1. *for any $1 \leq j \leq d$, $\sup_{p \geq 0} \pi_{p,0}(x_{0,1:j}) \leq C$, $\inf_{p \geq 0} \pi_{p,0}(x_{0,1:j}) \geq C'$,*
2. *for any $p \geq 1$, $\|\pi_{p,0} - \pi_{p-1,0}\|_{\text{tv}} \leq C\rho^{p-1}$,*
3. *for any $1 \leq j \leq d$, $p \geq 1$, $\sup_{x_{1:j} \in \mathbf{E}^j} \|\pi_{p,0}(\cdot|x_{1:j}) - \pi_{p-1,0}(\cdot|x_{1:j})\|_{\text{tv}} \leq C\rho^{p-1}$,*
4. *for any $p \geq 0$, $(x, x') \in \mathbf{X}^2$, $|\pi_{p,0}(x) - \pi_{p,0}(x')| \leq C|x - x'|$,*
5. *for any $p \geq 0$, $1 \leq j \leq d$, $(x_{1:j}, x'_{1:j}) \in (\mathbf{E}^j)^2$, $|\pi_{p,0}(x_{1:j}) - \pi_{p,0}(x'_{1:j})| \leq C|x_{1:j} - x'_{1:j}|$.*

Proof. Item 1 follows trivially from (A1) and the compactness of E .

Item 2 follows from the backward Markov chain representation of the smoother and (A1); see, for instance, [4] and the references therein.

To prove item 3, we first consider controlling for any fixed $1 \leq j \leq d$ $p \geq 1$,

$$|\pi_{p,0}(x_{1:j}) - \pi_{p-1,0}(x_{1:j})|.$$

Denoting $\pi_{(p)}$ as the filter at time p and setting for $k \geq 0$

$$B_k(x_{k+1}, x_k) = \frac{\pi_{(k)}(x_k)f(x_k, x_{k+1})}{\int_{\mathsf{X}} \pi_{(k)}(x_k)f(x_k, x_{k+1})dx_k}$$

we can write

$$(A.1) \quad |\pi_{p,0}(x_{1:j}) - \pi_{p-1,0}(x_{1:j})| \\ = \text{Osc}(B_0(\cdot, x_{1:j})) \left| [\pi_{(p)} B_{p-1} - \pi_{(p-1)}](B_{p-2:1}) \left(\frac{B_0(\cdot, x_{1:j})}{\text{Osc}(B_0(\cdot, x_{1:j}))} \right) \right|.$$

Using standard results for the total variation distance

$$|\pi_{p,0}(x_{1:j}) - \pi_{p-1,0}(x_{1:j})| \leq \text{Osc}(B_0(\cdot, x_{1:j})) \prod_{s=1}^{p-2} \omega(B_s),$$

where $\omega(B_s)$ is the Dobrushin coefficient of the Markov kernel B_s . Standard calculations yield that there exists a $\rho \in (0, 1)$ such that $\text{Osc}(B_0(\cdot, x_{1:j})) \vee \omega(B_s) \leq C\rho$, where C does not depend upon $x_{1:j}$. Hence we have shown that

$$(A.2) \quad \sup_{x_{1:j} \in \mathsf{E}^j} |\pi_{p,0}(x_{1:j}) - \pi_{p-1,0}(x_{1:j})| \leq C\rho^{p-1}.$$

To prove the result of interest we have for any $\varphi \in \text{Osc}_1(\mathsf{E})$

$$|\pi_{p,0}(\varphi|x_{1:j}) - \pi_{p-1,0}(\varphi|x_{1:j})| = \frac{1}{\pi_{p,0}(x_{1:j-1})} \int_{\mathsf{E}} \varphi(x_j)[\pi_{p,0}(x_{1:j}) - \pi_{p-1,0}(x_{1:j})]dx_j \\ + \frac{\pi_{p-1,0}(x_{1:j-1}) - \pi_{p,0}(x_{1:j-1})}{\pi_{p,0}(x_{1:j-1})\pi_{p-1,0}(x_{1:j-1})} \int_{\mathsf{E}} \varphi(x_j)\pi_{p-1,0}(x_{1:j})dx_j.$$

The conclusion then follows by using (A.2) and 1.

Item 4 follows almost immediately from (A2) and the definition of the smoother. Item 5 follows from 4 on marginalization and the compactness of E . \square

Proof of Theorem 2.1. Standard calculations for i.i.d. random variables and the Lipschitz property of φ clearly yield

$$\text{Var} \left[\frac{1}{N_p} \sum_{i=1}^N [\varphi(\Pi_{p,0}^{-1}(U^i)) - \varphi(\Pi_{p-1,0}^{-1}(U^i))] \right] \leq \frac{\|\varphi\|_{\text{Lip}}^2}{N_p} \int_{[0,1]} |\Pi_{p,0}^{-1}(u) - \Pi_{p-1,0}^{-1}(u)|^2 du.$$

Now we note that

$$\int_{[0,1]} |\Pi_{p,0}^{-1}(u) - \Pi_{p-1,0}^{-1}(u)|^2 du = W_2(\pi_{p,0}, \pi_{p-1,0})^2,$$

where $W_2(\pi_{p,0}, \pi_{p-1,0})$ is the 2-Wasserstein distance between $\pi_{p,0}$ and $\pi_{p-1,0}$. As X is compact it follows that

$$W_2(\pi_{p,0}, \pi_{p-1,0})^2 \leq \left(\int_X dx \right)^2 \|\pi_{p,0} - \pi_{p-1,0}\|_{\text{tv}},$$

where $\|\cdot\|_{\text{tv}}$ is the total variation distance. Under our assumptions one can show that there exists $\rho \in (0, 1)$, $C < +\infty$ such that for any $p \geq 1$ (see Lemma A.1 2., which holds when $d = 1$)

$$\|\pi_{p,0} - \pi_{p-1,0}\|_{\text{tv}} \leq C\rho^{p-1}.$$

The proof is then easily concluded. \square

LEMMA A.2. *Assume (A1–2). Then there exists $C < +\infty$, $\rho \in (0, 1)$ such that for any $p \geq 1$*

$$\mathbb{E}[|\xi_{p,d}^1 - \xi_{p-1,d}^1|^2] \leq C\rho^{p-1}.$$

Proof. The proof is by induction on d , the case $d = 1$ being proved by the approach in the proof of Theorem 2.1. Throughout C is a finite constant whose value may change from line-to-line, but does not depend upon p .

We suppose the result for $d - 1$ and consider d . For simplicity of notation, we drop the superscript 1 from the notation, e.g., we write $\xi_{p,d}$ instead of $\xi_{p,d}^1$. We have

$$\begin{aligned} \mathbb{E}[|\xi_{p,d} - \xi_{p-1,d}|^2] &= \mathbb{E}[\mathbb{E}[|\xi_{p,d}^1 - \xi_{p-1,d}^1|^2 | U_{1:d-1}]] \\ (A.3) \quad &\leq C\mathbb{E}[\|\pi_{p,0}(\cdot | \xi_{p,d-1}) - \pi_{p-1,0}(\cdot | \xi_{p-1,d-1})\|_{\text{tv}}], \end{aligned}$$

where, to go to the second line, we have used (conditional upon $U_{1:d}$) the relationship between the squared 2-Wasserstein distance and the (generalized) inverse CDF, along with the total variation bound as used in the proof of Theorem 2.1.

Now, we have

$$\begin{aligned} (A.4) \quad &\|\pi_{p,0}(\cdot | \xi_{p,d-1}) - \pi_{p-1,0}(\cdot | \xi_{p-1,d-1})\|_{\text{tv}} \\ &\leq \|\pi_{p,0}(\cdot | \xi_{p,d-1}) - \pi_{p-1,0}(\cdot | \xi_{p,d-1})\|_{\text{tv}} + \|\pi_{p-1,0}(\cdot | \xi_{p,d-1}) - \pi_{p-1,0}(\cdot | \xi_{p-1,d-1})\|_{\text{tv}}. \end{aligned}$$

By Lemma A.1 3. it follows that

$$(A.5) \quad \|\pi_{p,0}(\cdot | \xi_{p,d-1}) - \pi_{p-1,0}(\cdot | \xi_{p,d-1})\|_{\text{tv}} \leq C\rho^{p-1}$$

so we consider $\|\pi_{p-1,0}(\cdot | \xi_{p,d-1}) - \pi_{p-1,0}(\cdot | \xi_{p-1,d-1})\|_{\text{tv}}$. For any $\varphi \in \text{Osc}_1(E)$

$$\begin{aligned} &\pi_{p,0}(\varphi | \xi_{p,d-1}) - \pi_{p-1,0}(\varphi | \xi_{p,d-1}) \\ &= \frac{1}{\pi_{p-1,0}(\xi_{p-1,d-1})} \int_E \varphi(x) [\pi_{p-1,0}(\xi_{p,d-1}, x) - \pi_{p-1,0}(\xi_{p-1,d-1}, x)] dx \\ &\quad + \frac{\pi_{p-1,0}(\xi_{p-1,d-1}) - \pi_{p-1,0}(\xi_{p,d-1})}{\pi_{p-1,0}(\xi_{p,d-1}) \pi_{p-1,0}(\xi_{p-1,d-1})} \int_E \varphi(x) \pi_{p-1,0}(\xi_{p-1,d-1}, x) dx. \end{aligned}$$

Applying Lemma A.1 item 4 to the first term on the R.H.S. and Lemma A.1 item 5 to the second term on the R.H.S. along with the boundedness of φ and compactness of E , we have that

$$\begin{aligned} |\pi_{p,0}(\varphi | \xi_{p,d-1}) - \pi_{p-1,0}(\varphi | \xi_{p,d-1})| &\leq \frac{C}{\pi_{p-1,0}(\xi_{p-1,d-1})} |\xi_{p,d-1} - \xi_{p-1,d-1}| \\ &\quad + \frac{C}{\pi_{p-1,0}(\xi_{p,d-1}) \pi_{p-1,0}(\xi_{p-1,d-1})} |\xi_{p,d-1} - \xi_{p-1,d-1}|. \end{aligned}$$

Applying Lemma A.1 1. we can then establish that

$$(A.6) \quad \|\pi_{p-1,0}(\cdot|\xi_{p,d-1}) - \pi_{p-1,0}(\cdot|\xi_{p-1,d-1})\|_{\text{tv}} \leq C|\xi_{p,d-1} - \xi_{p-1,d-1}|.$$

Combining (A.5) and (A.6) with (A.4) and noting (A.3), we have shown that

$$\mathbb{E}[|\xi_{p,d} - \xi_{p-1,d}|^2] \leq C\left(\rho^{p-1} + \mathbb{E}[|\xi_{p,d-1} - \xi_{p-1,d-1}|]\right).$$

The proof is completed by using the Jensen inequality and the induction hypothesis. \square

Proof of Theorem 2.2. We have

$$\text{Var}\left[\frac{1}{N_p} \sum_{i=1}^{N_p} [\varphi(\xi_{p,d}^i) - \varphi(\xi_{p-1,d}^i)]\right] \leq \frac{\|\varphi\|_{\text{Lip}}^2}{N_p} \mathbb{E}[|\xi_{p,d}^1 - \xi_{p-1,d}^1|^2].$$

The proof is then completed by applying Lemma A.2. \square

Appendix B. Linear Gaussian result.

Proof of Theorem 4.1. The Rauch–Tung–Striebel smoother gives an expression of the smoothed mean $m_{p|n}$ and variance $v_{p|n}$ at time p given the observations y_0, \dots, y_n as

$$\begin{aligned} m_{p|n} &= m_{p|p} + c_p(m_{p+1|n} - m_{p+1|p}), \\ v_{p|n} &= v_{p|p} + c_p^2(v_{p+1|n} - v_{p+1|p}) \end{aligned}$$

with $c_p = \alpha m_{p|p}/m_{p+1|p}$, where $m_{p+1|p}$ and $v_{p+1|p}$ are the predicted mean and variance at time $p+1$ given the observations y_0, \dots, y_p . It follows that the mean m_p and variance v_p of $\pi_{p,0}$ satisfy similar relations to the filtered means and variances:

$$m_p = \sum_{i=0}^p m_{i|i} \alpha^i (1 - \mathbb{I}_{i < p} \alpha^2 d_p) \prod_{j=0}^{i-1} d_j \quad \text{and} \quad v_p = \sum_{i=0}^p v_{i|i} \alpha^{2i} (1 - \mathbb{I}_{i < p} \alpha^4 d_p^2) \prod_{j=0}^{i-1} d_j^2,$$

where $d_p = v_{p|p}/v_{p+1|p}$ and where \mathbb{I}_c is the indicator of condition c . The objective is to compute the order of

$$\Pi_{p,0}^{-1}(u) - \Pi_{p-1,0}^{-1}(u) = m_p - m_{p-1} + \sqrt{2} \operatorname{erf}^{-1}(2u-1)(\sigma_p - \sigma_{p-1}),$$

where $\sigma_p = \sqrt{v_p}$. From the above expression, it follows easily that

$$m_p - m_{p-1} = \alpha^p (m_{p|p} - m_{p|p-1}) \prod_{i=0}^{p-1} d_i \quad \text{and} \quad v_p - v_{p-1} = \alpha^{2p} (v_{p|p} - v_{p|p-1}) \prod_{i=0}^{p-1} d_i^2,$$

which yields the same order for both $m_p - m_{p-1}$ and $\sigma_p - \sigma_{p-1}$. The desired result follows from the fact that

$$\alpha^p \prod_{i=0}^{p-1} d_i = \alpha^p \prod_{i=0}^{p-1} \frac{v_{i|i}}{\alpha v_{i|i} + \beta^2} = \prod_{i=0}^{p-1} \frac{\alpha}{\alpha^2 + \beta^2/v_{i|i}} = \prod_{i=0}^{p-1} \left(\alpha + \frac{\beta^2}{\alpha v_{i|i}}\right)^{-1}$$

and from the assumption that $v_{p|p} = \text{Var}(X_p | y_{0:p}) \approx \gamma^2$ for all p large enough. \square

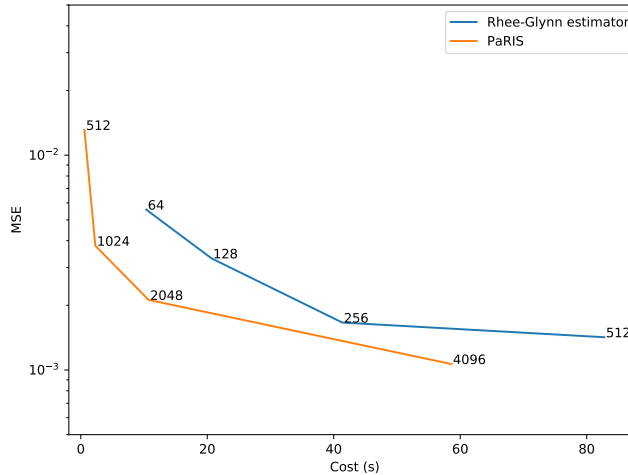


FIG. 4. Performance of the Rhee–Glynn estimator against the PaRIS algorithm with a linear-Gaussian model, averaged over 100 Monte Carlo simulations, where the number of samples is indicated on the figure. The reference for the computation of the MSE is the Rauch–Tung–Striebel smoother. The results for the Rhee–Glynn estimator are averaged over 2^{10} runs of the estimator.

Appendix C. The Rhee–Glynn smoothing estimator. We compare the so-called *Rhee–Glynn smoothing estimator* described in [16] with the PaRIS algorithm [22] on the linear-Gaussian model considered in section 4.1.2. The Rhee–Glynn smoothing estimator is implemented with ancestor sampling [21] and where all the generated paths are used in the estimate of $X_0 | y_{1:n^*}$, as originally suggested in [1] in the context of particle Markov chain Monte Carlo.

The result of the comparison is given in Figure 4, where it appears that the PaRIS algorithm slightly outperforms the Rhee–Glynn smoothing estimator. Although the scenario considered here is linear and Gaussian, none of the compared methods relies on these assumptions so that the conclusions made for this case are generalizable to some other classes of scenarios. This justifies the sole use of the PaRIS algorithm in section 4 for comparison against the proposed approach.

REFERENCES

- [1] C. ANDRIEU, A. DOUCET, AND R. HOLENSTEIN (2010), *Particle Markov chain Monte Carlo methods (with discussion)*, J. Roy. Statist. Soc. Ser. B, 72, pp. 269–342.
- [2] J. P. BOYD (2001), *Chebyshev and Fourier spectral methods*, Courier Corporation, North Chelmsford, MA.
- [3] P. BUNCH AND S. GODSILL (2016), *Approximations of the optimal importance density using Gaussian particle flow importance sampling*, J. Amer. Statist. Assoc., 111, pp. 748–762.
- [4] O. CAPPÉ, T. RYDEN, AND É. MOULINES (2005), *Inference in Hidden Markov Models*, Springer, New York.
- [5] N. CHOPIN, AND S. S. SINGH (2015), *On particle Gibbs sampling*, Bernoulli, 21, pp. 1855–1883.
- [6] F. DAUM AND J. HUANG (2008), *Particle flow for nonlinear filters with log-homotopy*, in Signal and Data Processing of Small Targets. International Society for Optics and Photonics, Bellingham, WA.
- [7] P. DEL MORAL, A. DOUCET, AND S. S. SINGH (2010), *A backward interpretation of Feynman–Kac formulae*, ESAIM Math. Model. Numer. Anal., 44, pp. 947–975.
- [8] A. DOUCET AND A. JOHANSEN (2011), *A tutorial on particle filtering and smoothing: Fifteen years later*, in *Handbook of Nonlinear Filtering*, D. Crisan and B. Rozovsky, eds., Oxford University Press, Oxford.

- [9] D. A. EDWARDS (2011), *On the Kantorovich-Rubinstein theorem*, *Expo. Math.*, 29, pp. 387–398.
- [10] M. B. GILES (2008), *Multilevel Monte Carlo path simulation*, *Oper. Res.*, 56, pp. 607–617.
- [11] M. B. GILES (2013), *Multilevel Monte Carlo methods*, in *Monte Carlo and Quasi-Monte Carlo Methods 2012*, Springer, New York, pp. 83–103.
- [12] A. GREGORY, C. J. COTTER, AND S. REICH (2016), *Multilevel ensemble transform particle filtering*, *SIAM J. Sci. Comput.*, 38(3), pp. A1317–A1338.
- [13] S. HEINRICH (2001), *Multilevel Monte Carlo methods*, in *Large-Scale Scientific Computing*, S. Margenov, J. Wasniewski, and P. Yalamov, eds., Springer, New York.
- [14] J. HENG, A. DOUCET, AND Y. POKERN (2015), *Gibbs Flow for Approximate Transport with Applications to Bayesian Computation*, <https://arxiv.org/abs/1509.08787>.
- [15] H. HOEL, K. J. LAW, AND R. TEMPONE (2016), *Multilevel ensemble Kalman filtering*, *SIAM J. Numer. Anal.*, 54, pp. 1813–1839.
- [16] P. JACOB, F. LINDSTEN, AND T. SCHÖN (2017), *Smoothing with Couplings of Conditional Particle Filters*, <https://arxiv.org/abs/1701.02002>.
- [17] A. JASRA (2015), *On the behaviour of the backward interpretation of Feynman-Kac formulae under verifiable conditions*, *J. Appl. Probab.*, 52, pp. 339–359.
- [18] A. JASRA, K. KAMATANI, K. J. H. LAW, AND Y. ZHOU (2017), *Multilevel particle filters*, *SIAM J. Numer. Anal.*, 55, pp. 3068–3096.
- [19] N. KANTAS, A. DOUCET, S. S. SINGH, J. M. MACIEJOWSKI, AND N. CHOPIN (2015), *On particle methods for parameter estimation in general state-space models*, *Statist. Sci.*, 30, pp. 328–351.
- [20] P. R. KUMAR AND V. PRAVIN (1986), *Stochastic Systems: Estimation, Identification, and Adaptive Control*, Prentice-Hall, Englewood Cliffs, NJ.
- [21] F. LINDSTEN, M. I. JORDAN, AND T. B. SCHÖN (2014), *Particle Gibbs with ancestor sampling*, *J. Mach. Learn. Res.*, 15, pp. 2145–2184.
- [22] J. OLSSON AND J. WESTERBORN (2017), *Efficient particle-based online smoothing in general hidden Markov models: The PaRIS algorithm*, *Bernoulli*, 23, pp. 1951–1996.
- [23] M. PARNO, T. MOSELHY, AND Y. MARZOUK (2016), *A multiscale strategy for Bayesian inference using transport maps*, *SIAM/ASA J. Uncertain. Quantif.*, 4, pp. 1160–1190.
- [24] H. E. RAUCH, C. STRIEBEL, AND F. TUNG (1965), *Maximum likelihood estimates of linear dynamical systems*, *AIAA J.*, 3, pp. 1445–1450.
- [25] C. H. RHEE AND P. W. GLYNN (2015), *Unbiased estimation with square root convergence for SDE models*, *Oper. Res.*, 63, pp. 1026–1043.
- [26] A. SPANTINI, D. BIGONI, AND Y. MARZOUK (2018), *Inference via low-dimensional couplings*, *J. Mach. Learn. Res.*, 19, pp. 2639–2709.